Research Square

Preprints are preliminary reports that have not undergone peer review.
They should not be considered conclusive, used to inform clinical practice,
or referenced by the media as validated information.

Singularity-Free Predefined-Time Sliding Mode Control With a Fixed-Time Extended State Observer for Robot Manipulators

NgocSon Vu

vungocson.haui.271199@gmail.com

Polytechnic College

VanCuong Pham

Hanoi University of Industry

HoangNha Phi

Hanoi University of Industry

TieuNien Le

East Asia University of Technology

KimThao Tran Thi

East Asia University of Technology

Research Article

Keywords: Predefined-time stability, sliding mode control, extended state observer, robot manipulators, singularity avoidance, chattering reduction

Posted Date: November 13th, 2026

DOI: https://doi.org/10.21203/rs.3.rs-11493879/v1

License: This work is licensed under a Creative Commons Attribution 4.0 International License.
Read Full License

Additional Declarations: No competing interests reported.

Original Paper

Singularity-Free Predefined-Time Sliding Mode Control With a Fixed-Time Extended State Observer for Robot Manipulators

NgocSon Vu[1,2*], VanCuong Pham[2], HoangNha Phi[2], TieuNien Le[3] and KimThao Tran Thi[3]

[1]Polytechnic College, Hoai Duc District, Hanoi, 100000, Hanoi, Vietnam.
[2]Hanoi University of Industry, No. 298 Cau Dien Street, Bac Tu Liem District, Hanoi, 100000, Hanoi, Vietnam.
[3]East Asia University of Technology, Trinh Van Bo Street, Nam Tu Liem District, Hanoi, 100000, Hanoi, Vietnam.
*Correspondence: vungocson.haui.271199@gmail.com

Abstract: In this paper, the trajectory tracking problem of robot manipulators subject to parametric uncertainties, unmodeled friction, external disturbances, and actuator saturation is addressed, with the requirement that the settling time be assigned directly by the designer. A singularity-free predefined-time sliding surface is constructed from a class of predefined-time stable systems whose settling-time function is given in the closed form $(2T_c/\pi)\arctan(|x_0|^p)$, so that the least upper bound of the settling time is defined by the user-selected parameter T_c. Near the origin, the fractional-power term responsible for the singularity is replaced by a C^1 quadratic transition function, by which the control signal is kept bounded. A predefined-time reaching law is then combined with a fixed-time extended state observer (FxESO), by which the lumped disturbance is estimated and compensated, so that only a small smooth robust term is required. It is proved that the tracking errors are driven into a small residual set within a time bounded by the observer convergence time plus two designer-selected constants. Simulations are carried out on a two-link manipulator, and the method is compared with conventional, nonsingular terminal, and fixed-time sliding mode controllers, including a smoothed fixed-time controller and an ablation without the observer. With the proposed controller, a lower steady-state error than that of the discontinuous fixed-time controller is achieved, while the total variation of the control torque is reduced by more than four orders of magnitude and the control energy is reduced by a factor of 7.8. Through initial-condition sweeps, it is confirmed that the prescribed bound on the settling time is never exceeded when the actuators are not saturated.
Keywords: Predefined-time stability, sliding mode control, extended state observer, robot manipulators, singularity avoidance, chattering reduction

1 Introduction

Robot manipulators are strongly coupled nonlinear systems; their dynamic parameters are changed by the payload, and their friction and environmental disturbances are difficult to model [1, 2]. In this context, sliding mode control (SMC) is regarded as attractive, since the closed loop is rendered insensitive to matched uncertainties [1]. Its main drawbacks are the chattering caused by a discontinuous switching term, whose gain is required to exceed the disturbance bound [26], and the merely asymptotic convergence of the tracking error obtained with the conventional linear surface.

In terminal sliding mode control, fractional powers are introduced so that finite-time convergence is obtained, and the singularity of the original design for rigid manipulators is removed by the nonsingular terminal sliding mode (NTSM) of [3]. However, the settling time of finite-time schemes is not bounded with respect to the initial error. This dependence is removed by fixed-time stability [4, 5]: the settling time is bounded by a constant that is valid for all initial conditions. Several fixed-time sliding mode controllers combined with fixed-time disturbance observers have been reported for manipulators [22–24]. However, the settling-time bound of fixed-time systems is determined by several controller gains and is known to be conservative [6]; hence, a desired convergence time cannot be imposed unless that function is inverted and a pessimistic estimate is accepted.

In predefined-time stability [7, 8], a further step is taken: the upper bound of the settling time is given explicitly by a single design parameter. Predefined-time terminal sliding mode controllers for manipulators were proposed in [10] and [11], and adaptive neural [12], fractional-order [13], and observer-based [15] variants were subsequently developed. In a related line of work, prescribed-time control [9], time-varying gains are employed, which are increased without bound as the prescribed instant is approached; in recent results, this conservatism is reduced and the input is kept bounded [14]. Despite this progress, three practical issues have not been sufficiently addressed. First, terms such as $\mathrm{sig}^{1-p}(e)$, whose derivative is unbounded at $e = 0$, are contained in many predefined-time surfaces, and the remedies based on switching or saturation functions are often non-smooth. Second, robustness is usually obtained through a switching gain larger than the disturbance bound, by which chattering is reintroduced. Alternatively, the lumped disturbance can be estimated and cancelled by extended state observers [16], and fixed-time observers and differentiators based on bi-limit homogeneity or uniform exact differentiation have been developed [17–21]; however, they have mostly been combined

with fixed-time rather than predefined-time controllers for manipulators [22–24]. Third, the interaction between the predefined-time bound and actuator saturation has rarely been quantified, and comparisons with smoothed baselines have seldom been made; therefore, it has not been clarified whether a reported chattering reduction is caused by the control structure or merely by the replacement of $\mathrm{sign}(\cdot)$ with a continuous approximation.

To address these issues, a predefined-time sliding mode controller with a fixed-time extended state observer (PTSMC-FxESO) is proposed in this paper. The main contributions are summarized as follows.

(1) A singularity-free predefined-time sliding surface is designed from a class of predefined-time stable systems with the closed-form settling-time function $(2T_c/\pi)\arctan(|x_0|^p)$. Therefore, the least upper bound of the settling time, rather than a conservative estimate, is given by the parameter T_c. The singularity is removed by a C^1 quadratic transition function, while the derivative of the surface is kept uniformly bounded.

(2) A predefined-time reaching law is combined with an FxESO in which the actually applied (saturated) torque is used. Since the lumped disturbance is compensated by the observer, a small and smooth robust term is sufficient. The resulting practical predefined-time stability is proved with an explicit time budget $T_o + T_{c2} + T_{c1}/(1-\theta)$ and an explicit residual set.

(3) An extensive simulation study is reported, in which a smoothed fixed-time controller is included as a fair baseline, and an ablation without the observer, initial-condition and predefined-time sweeps, measurement-noise tests, and Monte Carlo tests are performed. In addition, the actuator-feasibility condition under which the predefined-time bound is guaranteed is identified.

Compared with the closely related observer-based design in [15], in which a predefined-time disturbance observer is combined with prescribed performance functions, emphasis is placed in this work on the tightness of the time bound, on a smooth singularity-avoidance mechanism, and on a quantitative assessment of chattering, robustness, and saturation effects.

The remainder of the paper is organized as follows. The preliminaries and the problem formulation are given in Section 2. The observer, the sliding surface, the control law, and the stability analysis are presented in Section 3. The simulation results are reported in Section 4, and conclusions are drawn in Section 5.

2 Preliminaries and Problem Formulation

2.1 Notation

For $x \in \mathbb{R}$ and $a > 0$, $\mathrm{sig}^a(x)$ is defined as $|x|^a\mathrm{sign}(x)$. For vectors, $\mathrm{sig}^a(\cdot)$, $\tanh(\cdot)$, and $|\cdot|^a$ are applied elementwise, and the elementwise product is denoted by $\odot$. The Euclidean norm is denoted by $\|\cdot\|$.

2.2 Robot Dynamics

The dynamics of an n-link rigid manipulator are described by

$$M(q)\ddot{q} + C(q,\dot{q})\dot{q} + G(q) + F(\dot{q}) + \tau_d(t) = \mathrm{sat}(\tau_c) \tag{1}$$

where $q \in \mathbb{R}^n$ is the joint position, $M(q)$ is the symmetric positive-definite inertia matrix, the Coriolis and centripetal torques are contained in $C(q,\dot{q})\dot{q}$, $G(q)$ is the gravity vector, $F(\dot{q})$ is the friction torque, $\tau_d(t)$ is an external disturbance, τ_c is the commanded torque, and each component of τ_c is limited to $[-\tau_{\max,i}, \tau_{\max,i}]$ by $\mathrm{sat}(\cdot)$. The matrix $\dot{M} - 2C$ is skew-symmetric [2].

Only the nominal matrices M_0, C_0, and G_0 are known to the controller. With $\tau = \mathrm{sat}(\tau_c)$, (1) is rewritten as

$$\ddot{q} = f_0(q,\dot{q}) + M_0^{-1}\tau + D(t), \qquad f_0 = -M_0^{-1}(C_0\dot{q} + G_0) \tag{2}$$

where the lumped disturbance, in which parametric uncertainty, friction, and external disturbances are collected, is given by

$$D = M^{-1}(\tau - C\dot{q} - G - F - \tau_d) - M_0^{-1}(\tau - C_0\dot{q} - G_0). \tag{3}$$

Assumption 1 $D(t)$ is assumed to be continuously differentiable, and unknown constants $\bar{D}$ and L are assumed to exist such that $\| D \| \leq \bar{D}$ and $\| \dot{D} \| \leq L$.

Assumption 2 The reference $q_d(t)$ and its first two derivatives are assumed to be continuous and bounded.

The tracking errors are defined as $e = q - q_d$ and $\dot{e} = \dot{q} - \dot{q}_d$. The control torque τ_c is to be designed such that e is driven into a small neighborhood of the origin within a time whose upper bound is selected a priori by the designer, independently of $e(0)$.

2.3 Predefined-Time Stability

Lemma 1 *Let* $0 < p < 1$ *and* $T_c > 0$*, and let the following system be considered:*

$$\dot{x} = -\Psi_{p,T_c}(x), \qquad \Psi_{p,T_c}(x) = \frac{\pi}{2pT_c}[\mathrm{sig}^{1-p}(x) + \mathrm{sig}^{1+p}(x)]. \tag{4}$$

Then, the origin is reached by every solution at the time

$$T(x_0) = \frac{2T_c}{\pi}\arctan(|x_0|^p) < T_c \tag{5}$$

and $\sup_{x_0} T(x_0) = T_c$ *is satisfied.*

Proof Let $y = |x|$ and $w = y^p$. For $y > 0$, $\dot{y} = -\frac{\pi}{2pT_c}(y^{1-p} + y^{1+p})$ is obtained, and hence $\dot{w} = p\,y^{p-1}\dot{y} = -\frac{\pi}{2T_c}(1 + w^2)$. By integration from $w(0) = |x_0|^p$ to $w = 0$, (5) is obtained. Since $\arctan(\cdot) < \pi/2$ and $\arctan(w_0) \to \pi/2$ as $w_0 \to \infty$, the supremum is equal to T_c. □

System (4) is included in the class studied in [7, 8]. It is shown by Lemma 1 that T_c is the least upper bound of the settling time; this property is not shared by the gain-dependent bounds of fixed-time systems [4, 6].

Lemma 2 *Let* $\dot{x} = -\Psi_{p,T_c}(x) - \eta\tanh(x/\delta) + d(t)$ *be considered, with* $|d(t)| \le \varpi < \eta$ *and* $\delta > 0$*. Then, for any* x_0*,* $|x(t)| \le \bar{x} := \delta\,\mathrm{artanh}(\varpi/\eta)$ *is satisfied for all* $t \ge T_c$*, and this set is forward invariant.*

Proof Let $V = |x|$. Whenever $V > \bar{x}$, $\eta\tanh(V/\delta) > \varpi$ is satisfied; hence, the upper right Dini derivative is bounded as $D^+V \le -\Psi_{p,T_c}(V) - (\eta\tanh(V/\delta) - \varpi) \le -\Psi_{p,T_c}(V)$. By the comparison lemma [25] and Lemma 1, the interval $[0, \bar{x}]$ is entered by V before T_c. On the boundary $V = \bar{x}$, $D^+V \le -\Psi_{p,T_c}(\bar{x}) < 0$ is obtained, by which the invariance is established. □

3 Controller Design

The overall structure is shown in Fig. 1. Since the analysis is carried out joint by joint, the design can be applied to any number of joints.

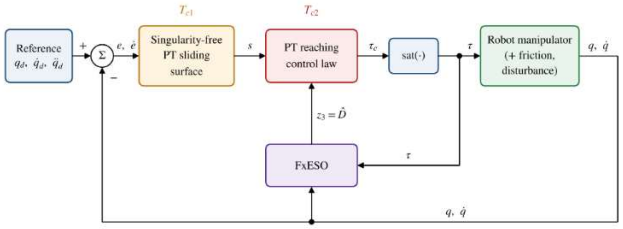


Fig. 1 Structure of the proposed PTSMC-FxESO controller. The time parameters T_{c1} and T_{c2} are selected by the designer

3.1 Fixed-Time Extended State Observer

D is treated as an extended state of (2), and the measured velocity is used; the FxESO is thus designed as

$$\begin{aligned} e_o &= \dot{q} - z_2 \\ \dot{z}_2 &= f_0 + M_0^{-1}\tau + z_3 + \beta_1[\mathrm{sig}^{\alpha}(e_o) + \mathrm{sig}^{\gamma}(e_o)] \\ \dot{z}_3 &= \beta_2[\mathrm{sig}^{2\alpha-1}(e_o) + \mathrm{sig}^{2\gamma-1}(e_o)] \end{aligned} \tag{6}$$

with $\alpha \in (1/2, 1)$, $\gamma > 1$, and $\beta_1, \beta_2 > 0$, where τ is the torque applied after saturation, so that the clipped part of τ_c is not misinterpreted as a disturbance.

Lemma 3 ([17, 18, 21]) *Under Assumption 1, if* α *and* γ *are chosen sufficiently close to one and* β_1, β_2 *are suitably selected, a time* T_o *independent of the initial estimation error and a constant* $\varpi > 0$*, which is decreased as the observer gains are increased, can be found such that* $|e_{D,i}(t)| \le \varpi$ *is satisfied for all* $t \ge T_o$*, where* $e_D = D - z_3$ *denotes the estimation error. If* $\dot{D} = 0$*, exact convergence is obtained.*

Observer (6) is homogeneous in the bi-limit [17]: finite-time convergence near the origin is ensured by the low-degree terms, and a uniform bound on the convergence time for large initial errors is ensured by the high-degree terms.

3.2 Singularity-Free Predefined-Time Sliding Surface

The sliding variable is defined for each joint as

$$s = \dot{e} + k_1[\varphi(e) + \mathrm{sig}^{1+p_1}(e)] = \dot{e} + \Phi_1(e), \qquad k_1 = \frac{\pi}{2p_1T_{c1}} \tag{7}$$

where $0 < p_1 < 1$ and $T_{c1} > 0$. On $s = 0$ and for $|e_i| \geq \varepsilon$, $\dot{e}_i = -\Psi_{p_1,T_{c1}}(e_i)$ is recovered; thus, Lemma 1 can be applied. Since the derivative of $\mathrm{sig}^{1-p_1}(e)$ is unbounded at $e = 0$, φ is defined as follows so that this singularity is avoided:

$$\varphi(e) = \begin{cases} \mathrm{sig}^{1-p_1}(e), & |e| \geq \varepsilon \\ l_1 e + l_2 e|e|, & |e| < \varepsilon \end{cases} \tag{8}$$

$$l_1 = (1+p_1)\varepsilon^{-p_1}, \qquad l_2 = -p_1\varepsilon^{-p_1-1} \tag{9}$$

where $\varepsilon > 0$ is a small constant. By the coefficients (9), the continuity of φ and φ' at $|e| = \varepsilon$ is ensured, so $\varphi \in C^1$. Moreover, φ is odd and strictly increasing, and the following bound is satisfied for $|e| < \varepsilon$:

$$0 < (1-p_1)\varepsilon^{-p_1} \leq \varphi'(e) \leq (1+p_1)\varepsilon^{-p_1} \tag{10}$$

whereas $0 < \varphi'(e) \leq (1-p_1)\varepsilon^{-p_1}$ is satisfied for $|e| \geq \varepsilon$. Hence, the derivative of the surface, given by

$$\dot{s} = \ddot{e} + {\Phi_1}'(e) \odot \dot{e}, \qquad {\Phi_1}'(e) = k_1[\varphi'(e) + (1+p_1)|e|^{p_1}] \tag{11}$$

is free of singularity and is bounded for bounded $(e, \dot{e})$.

3.3 Predefined-Time Control Law

By substituting (2) into (11), $\dot{s} = f_0 + M_0^{-1}\tau + D - \ddot{q}_d + {\Phi_1}'(e) \odot \dot{e}$ is obtained. The commanded torque is designed as

$$\tau_c = M_0\left[\ddot{q}_d - {\Phi_1}'(e) \odot \dot{e} - z_3 - \Psi_{p_2,T_{c2}}(s) - \eta\tanh(s/\delta)\right] + C_0\dot{q} + G_0 \tag{12}$$

where $0 < p_2 < 1$, $T_{c2} > 0$, $\eta > 0$, and $\delta > 0$. In the absence of saturation, the closed loop is reduced to

$$\dot{s} = -\Psi_{p_2,T_{c2}}(s) - \eta\tanh(s/\delta) + e_D. \tag{13}$$

3.4 Stability Analysis

Assumption 3 For $t \geq T_o$, the commanded torque is assumed to satisfy $|\tau_{c,i}| \leq \tau_{\max,i}$.

Theorem 1 *Let system (1) be considered under Assumptions 1–3, with observer (6), surface (7)–(9), and control law (12), where $\eta > \varpi$ is selected. Let $\bar{s} = \delta\,\mathrm{artanh}(\varpi/\eta)$. Then, for any $\theta \in (0,1)$ and any initial condition, each tracking error e_i is driven into, and is kept in, the set*

$$\Omega_e = \{|e_i| \leq \bar{e}\}, \qquad \bar{e} = \max\{\varepsilon,\ \Phi_1^{-1}(\bar{s}/\theta)\} \tag{14}$$

within the time

$$T \leq T_o + T_{c2} + \tfrac{T_{c1}}{1-\theta}. \tag{15}$$

Proof Step 1 (no finite escape on $[0, T_o]$). With $V_k = \frac{1}{2}\dot{q}^\top M\dot{q}$ and the skew symmetry of $\dot{M} - 2C$, $\dot{V}_k = \dot{q}^\top(\tau - G - F - \tau_d)$ is obtained. Since τ is saturated, G is bounded, and $\dot{q}^\top F(\dot{q}) \geq 0$ is satisfied for dissipative friction, $\dot{V}_k \leq c \parallel \dot{q} \parallel \leq c'\sqrt{V_k}$ is obtained for some constants c, c'. Thus, the growth of $\sqrt{V_k}$ is bounded by a linear function, and q and $\dot{q}$ are kept bounded on any finite interval. The boundedness of the observer error is guaranteed by Lemma 3.

Step 2 (reaching phase). For $t \geq T_o$, Assumption 3 is satisfied, and the hypothesis of Lemma 2 is satisfied by each component of (13) with $|e_{D,i}| \leq \varpi < \eta$. Hence, $|s_i(t)| \leq \bar{s}$ is guaranteed for all $t \geq T_o + T_{c2}$.

Step 3 (sliding phase). From (7), $\dot{e}_i = -\Phi_1(e_i) + s_i$ is obtained, where Φ_1 is odd and strictly increasing. Let $V = |e_i|$. Then, $D^+V \leq -\Phi_1(V) + \bar{s}$ is obtained. Whenever $\Phi_1(V) \geq \bar{s}/\theta$, $D^+V \leq -(1-\theta)\Phi_1(V)$ is satisfied. For $V \geq \varepsilon$, $(1-\theta)\Phi_1(V) = \Psi_{p_1,T_{c1}/(1-\theta)}(V)$; thus, by Lemma 1 and the comparison lemma, V is decreased to $\bar{e}$ within $T_{c1}/(1-\theta)$. The invariance of Ω_e is established as in Lemma 2. By combining the three steps, (14) and (15) are obtained. □

Remark 1 (tightness of the bound) As exact estimation is approached ($\varpi \to 0$), θ can be chosen arbitrarily small, and bound (15) is reduced to $T_o + T_{c2} + T_{c1}$, where T_{c1} and T_{c2} are least upper bounds by Lemma 1. For the fixed-time surface $\dot{e} = -a_1\mathrm{sig}^m(e) - a_2\mathrm{sig}^n(e)$, the classical bound $1/\big(a_1(1-m)\big) + 1/\big(a_2(n-1)\big)$ [4] is generally not attained, and a desired time cannot be assigned through a single parameter.

Remark 2 (singularity and boundedness) From (10), ${\Phi_1}'(e)$ is bounded by $k_1[(1+p_1)\varepsilon^{-p_1} + (1+p_1)|e|^{p_1}]$, so (12) is bounded for bounded states. Exactness is traded for smoothness through the parameter ε; inside $|e_i| < \varepsilon$, convergence of the error is still obtained, but at a rate determined by l_1.

Remark 3 (actuator feasibility) Assumption 3 is regarded as essential. If T_{c1} and T_{c2} are chosen too small with respect to $\tau_{\max}$ and the initial error, the required torque is saturated, and bound (15) may be violated. This effect is quantified in Section 4.5.

Remark 4 (tuning) T_{c1} and T_{c2} are selected according to the time specification and the available torque; the transient is shaped by $p_1, p_2 \in (0,1)$; estimation speed is traded against noise sensitivity through β_1, β_2; and smoothness is traded against residual error through δ. Since most of D is removed by z_3, η is only required to exceed the small residual ϖ.

4 Simulation Results

4.1 Setup

A planar two-link manipulator with point masses at the link tips is considered [2], and its parameters are listed in Table 1. The nominal masses used by all controllers are set 20% lower than the true masses. Viscous and Coulomb friction, $F(\dot{q}) = F_v\dot{q} + F_c\tanh(20\dot{q})$, is included only in the plant. The external disturbance is set to $\tau_d = [2\sin 2t + 0.5,\ 1.5\cos 2t]^{\mathrm{T}}$ N·m, and a load step of $[3,\ 2]^{\mathrm{T}}$ N·m is applied at $t = 5$ s. The reference is given by $q_d = [\sin t,\ \cos t]^{\mathrm{T}}$ rad, and the initial state is set to $q(0) = [0.5,\ 0.3]^{\mathrm{T}}$ rad and $\dot{q}(0) = 0$. The simulations are implemented in MATLAB with fixed-step Euler integration and a step size of 10^{-4} s, and the controller is updated at every step.

Table 1 Manipulator parameters

Parameter	True value	Nominal value
m_1, m_2 (kg)	1.0, 1.0	0.8, 0.8
l_1, l_2 (m)	1.0, 0.8	1.0, 0.8
F_v (N·m·s/rad), F_c (N·m)	0.5, 0.3	–
$\tau_{\max}$ (N·m)	[80, 40]	[80, 40]

In the proposed controller, $p_1 = p_2 = 0.5$, $T_{c1} = 1$ s, $T_{c2} = 0.5$ s, $\varepsilon = 0.01$, $\eta = 1$, $\delta = 0.02$, $\alpha = 0.8$, $\gamma = 1.2$, $\beta_1 = 120$, and $\beta_2 = 3600$ are used. The proposed controller is compared with the controllers listed in Table 2. The switching gain $K = 20$ of the baselines is chosen larger than the bound of the lumped disturbance, which is the standard means by which robustness is obtained without an observer. In FxTSMC, the same singularity-free transition function (8) is used, and its theoretical settling-time bound is calculated as 2.13 s. In the smoothed FxTSMC, $\mathrm{sign}(s)$ is replaced by $\tanh(s/0.02)$, so that the effect of smoothing is isolated. In the ablation "PTSMC w/o ESO," z_3 is set to zero and η is increased to 15.

Table 2 Baseline controllers

Method	Sliding variable and reaching law
SMC [1]	$s = \dot{e} + 5e$, $\dot{s} = -K\mathrm{sign}(s)$
NTSMC [3]	$s = e + \frac{1}{5}\mathrm{sig}^{5/3}(\dot{e})$, Feng–Yu–Man law
FxTSMC [4, 5]	$s = \dot{e} + 3\mathrm{sig}^{0.5}(e) + 3\mathrm{sig}^{1.5}(e)$, $\dot{s} = -5\mathrm{sig}^{0.5}(s) - 5\mathrm{sig}^{1.5}(s) - K\mathrm{sign}(s)$
FxTSMC (tanh)	As FxTSMC, with $\tanh(s/0.02)$
PTSMC w/o ESO	Proposed law with $z_3 = 0$, $\eta = 15$

The following metrics are used: the settling time T_s (last instant with $|e_i| > 0.01$ rad before the load step), $\mathrm{ITAE} = \int t|e_i|dt$, the maximum steady-state error $\mathrm{SS}_{\max}$ after the load step ($t > 6$ s), the control energy $E_i = \int \tau_i^2 dt$, and the total variation $\mathrm{TV}_i = \sum_k |\tau_i(k+1) - \tau_i(k)|$, which is adopted as a quantitative chattering index.

4.2 Tracking Under Uncertainty and Disturbances

The tracking errors are shown in Fig. 2, the control torques are shown in Fig. 3, and the metrics are summarized in Table 3.

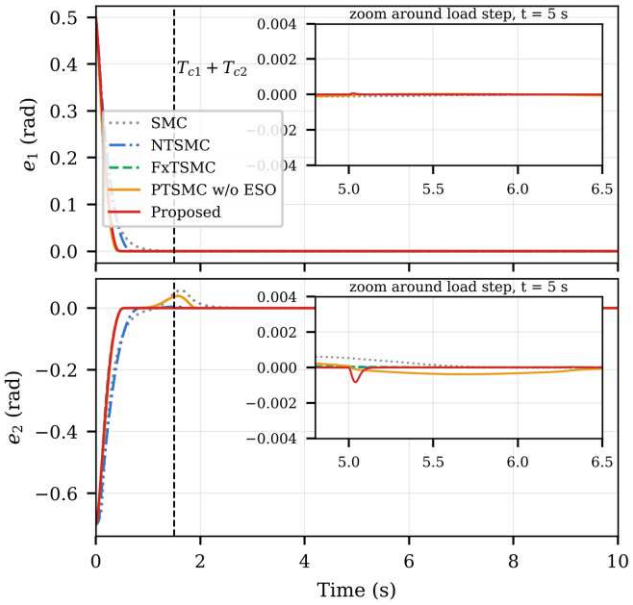


Fig. 2 Tracking errors of the two joints. $T_{c1} + T_{c2} = 1.5$ s is marked by the dashed line, and the response to the load step at $t = 5$ s is shown in the insets

Table 3 Performance metrics (joint 1 / joint 2)

Method	T_s (s)	ITAE ($\times 10^{-2}$)	$\mathrm{SS}_{\max}$ ($\times 10^{-5}$ rad)	E_1 ($\times 10^{3}$)	TV_1
SMC	0.78/2.07	2.33/10.38	11.0/55.9	36.9	8.5×10^6
NTSMC	0.57/0.73	1.70/4.29	0.17/1.78	37.6	8.5×10^6
FxTSMC	0.37/0.46	0.80/1.88	1.50/7.81	37.3	8.6×10^6
FxTSMC (tanh)	0.37/1.59	1.06/3.36	16.6/48.5	5.03	252
PTSMC w/o ESO	0.36/1.82	1.09/5.87	21.3/129.6	4.97	244
Proposed	**0.39/0.46**	**0.92/1.83**	**0.39/2.23**	**4.81**	**168**

Convergence within about 0.8 s is achieved by all methods except SMC, and convergence within the prescribed time $T_{c1} + T_{c2} = 1.5$ s is achieved by the proposed controller at both joints. A convergence speed comparable to that of FxTSMC is obtained; hence, the advantage of the proposed method is to be found elsewhere. Chattering between the saturation limits is exhibited by the three discontinuous controllers throughout the run (Fig. 3), with $\mathrm{TV}_1 \approx 8.5 \times 10^6$ N·m. A smooth torque with $\mathrm{TV}_1 = 168$ N·m is produced by the proposed controller, which corresponds to a reduction of about 51,000 times with respect to FxTSMC, and the control energy is reduced by a factor of 7.8. A peak torque of 39.7 N·m, about half of the limit, is required by the proposed controller, whereas 80 N·m is reached by all discontinuous controllers. At the same time, steady-state errors after the load step (3.9×10^{-6} and 2.2×10^{-5} rad) lower than those of FxTSMC are obtained. A similar steady-state accuracy is attained by NTSMC, but only at the cost of the same severe chattering and a slower transient.

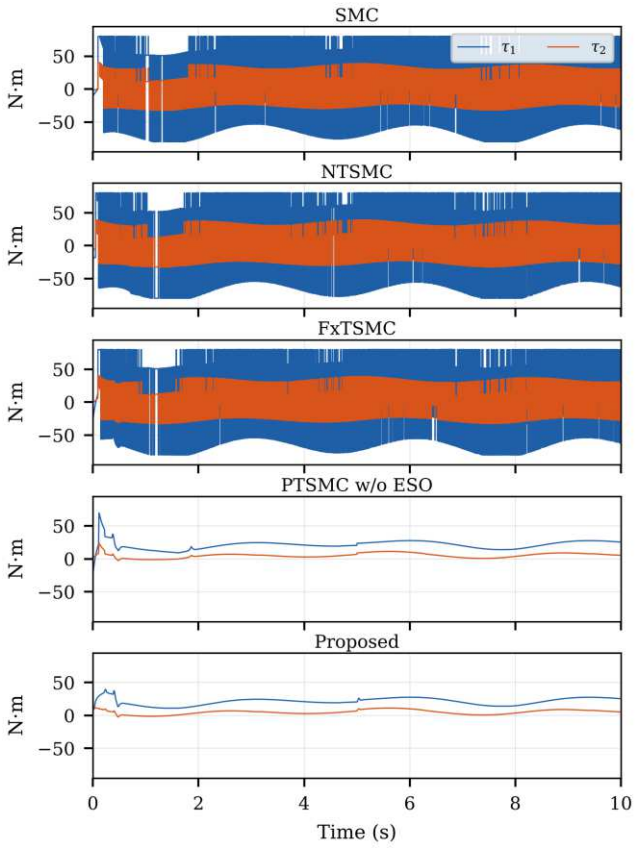


Fig. 3 Control torques. The torque is switched between the saturation limits by the three controllers with $\mathrm{sign}(\cdot)$, whereas smooth torques are produced by both PTSMC variants

4.3 Role of the Observer

As shown in Fig. 4, the lumped disturbance, including the jump caused by the load step, is tracked by z_3. When the observer is removed (Table 3, "PTSMC w/o ESO"), the steady-state error is increased by factors of 55 and 58 at joints 1 and 2, respectively, even though η is raised from 1 to 15. More importantly, the settling time of joint 2 is increased to 1.82 s, by which the prescribed bound of 1.5 s is exceeded. Therefore, the observer is required for the predefined-time property to be preserved with a smooth control law.

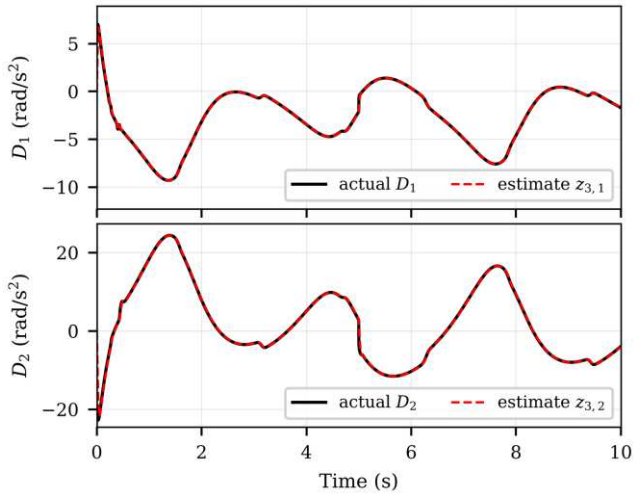


Fig. 4 Lumped disturbance D and its estimate z_3 obtained by the FxESO

4.4 Comparison With a Smoothed Fixed-Time Controller

When $\mathrm{sign}(s)$ is replaced by $\tanh(s/\delta)$ in FxTSMC, its chattering is reduced to the level of the proposed controller ($\mathrm{TV}_1 = 252$ N·m). However, its steady-state error is increased by factors of 43 and 22 at joints 1 and 2, respectively, relative to the proposed method, and the settling time of joint 2 is increased to 1.59 s. Therefore, the chattering reduction of the proposed controller cannot be attributed to smoothing alone; it is obtained by combining disturbance compensation with the predefined-time reaching law.

4.5 Verification of the Predefined-Time Property

Six initial errors with norms ranging from 0.28 to 3.61 rad are tested (Fig. 5 and Table 4). For the proposed controller, the settling time is increased only from 0.28 to 0.90 s and is always kept below 1.5 s. The settling time of NTSMC is increased with the initial error, and a value of 1.88 s is reached. The settling time of FxTSMC is also bounded; however, its theoretical bound of 2.13 s is 2.3 times larger than its largest observed value and cannot be assigned directly.

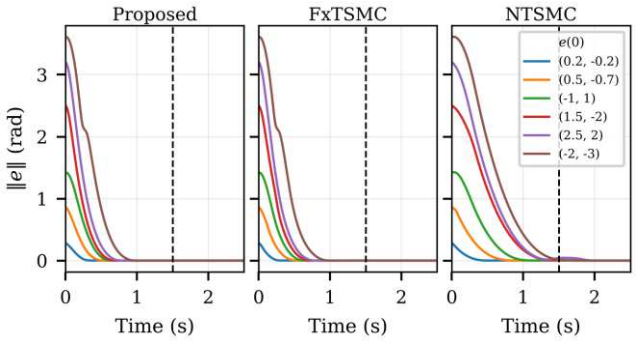


Fig. 5 Norm of the tracking error for six initial errors. $T_{c1} + T_{c2} = 1.5$ s is marked by the dashed line

Table 4 Settling time $\max(T_{s1}, T_{s2})$ (s) for different initial errors

$e(0)$ (rad)	$\| e(0) \|$	Proposed	FxTSMC	NTSMC
(0.2, −0.2)	0.28	0.28	0.24	0.37
(0.5, −0.7)	0.86	0.46	0.46	0.73
(−1, 1)	1.41	0.58	0.58	0.98
(1.5, −2)	2.50	0.63	0.66	1.31
(2.5, 2)	3.20	0.71	0.72	1.88
(−2, −3)	3.61	0.90	0.91	1.50

The effect of the predefined times is shown in Fig. 6 for the worst initial error. For $T_{c1} + T_{c2} = 1.5$ s and 3 s, settling times of 0.90 s and 1.33 s are observed, both within the bound, and slower convergence is obtained as intended. For $T_{c1} + T_{c2} = 0.75$ s, the 80 N·m limit is exceeded by the required torque during the initial transient, and the bound is violated by the observed settling time of 0.90 s. Thus, Remark 3 is confirmed: the predefined-time guarantee is valid only if the torque demanded by the prescribed time can be delivered by the actuators.

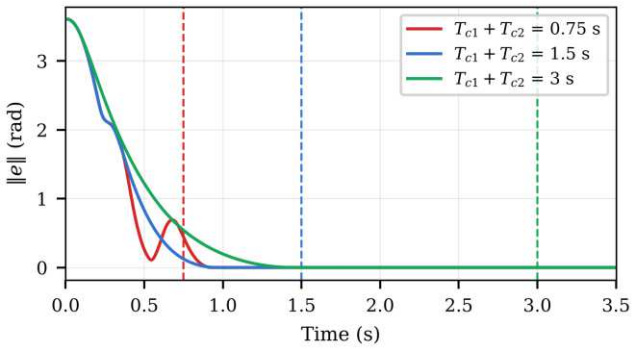


Fig. 6 Norm of the tracking error for three values of $T_{c1} + T_{c2}$ with $e(0) = (-2, -3)$ rad. The bounds are marked by dashed lines

4.6 Measurement Noise

Gaussian noise with standard deviations of 10^{-4} rad and 10^{-3} rad/s is added to the measured positions and velocities used by all controllers and by the observer (Table 5). The lowest steady-state RMSE and the lowest torque variation are obtained with the proposed controller. However, the total variation of every controller is increased by the noise, and that of the proposed controller is increased to 3.1×10^5 N·m. When the observer gains are reduced to $\beta_1 = 40$ and $\beta_2 = 400$, this value is barely changed (2.9×10^5 N·m), but the RMSE is increased to 5.3×10^{-4} rad. From this result, it can be inferred that the noise amplification is caused mainly by the steep fractional-power terms near the origin rather than by the observer; therefore, measurement filtering is suggested as a direction for future work.

Table 5 Results under measurement noise (sum over joints)

Method	Steady-state RMSE (rad)	TV (N·m)
SMC	1.6×10^{-3}	1.0×10^7
NTSMC	7.9×10^{-5}	8.4×10^6
FxTSMC	8.8×10^{-5}	8.9×10^6
FxTSMC (tanh)	2.1×10^{-4}	2.2×10^6
Proposed	$\mathbf{6.7 \times 10^{-5}}$	$\mathbf{3.1 \times 10^5}$

4.7 Monte Carlo Study

Thirty runs are performed, in which the true masses are drawn uniformly from $[0.76,\ 1.24]$ kg and the initial errors are drawn uniformly from $[-2,\ 2]$ rad (Fig. 7 and Table 6). A maximum settling time of 0.83 s is obtained with the proposed controller, which is below the 1.5 s bound in every run, whereas values of 2.58, 2.17, and 1.82 s are reached by SMC, NTSMC, and FxTSMC (tanh), respectively. In terms of the steady-state RMSE, in which the transient after the load step is included, the highest accuracy is achieved by FxTSMC with $\mathrm{sign}(\cdot)$, at the cost of an approximately 19,000 times larger torque variation. Among the smooth controllers, an RMSE 2.2 times lower than that of FxTSMC (tanh) is obtained with the proposed controller, and the smallest standard deviation among all methods is also obtained, from which the lowest sensitivity to parameter variation is inferred.

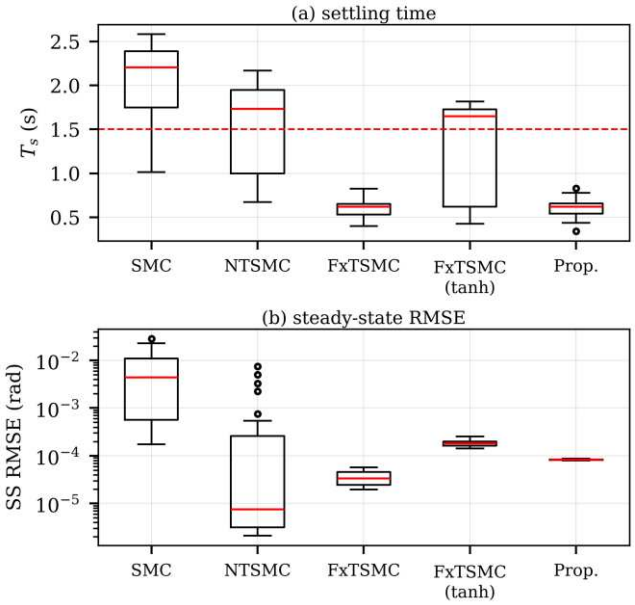


Fig. 7 Monte Carlo results over 30 runs: (a) settling time, where 1.5 s is marked by the dashed line; (b) steady-state RMSE (logarithmic scale)

Table 6 Monte Carlo results (30 runs)

Method	Mean / max T_s (s)	RMSE mean ± std ($\times 10^{-5}$ rad)	Mean TV (N·m)
SMC	2.02 / 2.58	707 ± 762	6.6×10^6
NTSMC	1.48 / 2.17	67.8 ± 167	6.8×10^6

Method	Mean / max T_s (s)	RMSE mean ± std ($\times 10^{-5}$ rad)	Mean TV (N·m)
FxTSMC	0.61 / 0.83	3.51 ± 1.12	6.7×10^6
FxTSMC (tanh)	1.23 / 1.82	18.3 ± 2.55	415
Proposed	**0.60 / 0.83**	**8.30 ± 0.20**	**356**

4.8 Discussion and Limitations

Three conclusions are supported by the results. First, the convergence time is assigned directly through T_{c1} and T_{c2} and is respected under various initial conditions and parameter variations, provided that the actuators are not saturated after the convergence of the observer. Second, when the lumped disturbance is compensated by the FxESO, an accuracy comparable to that of discontinuous high-gain designs is achieved with a smooth control law, while chattering is reduced by orders of magnitude and the energy consumption is reduced several times. Third, this combination cannot be provided by smoothing alone, as demonstrated by the smoothed FxTSMC. The main limitations are identified as the dependence of the bound on the actuator capacity, the sensitivity of the fractional-power terms to measurement noise, and the practical (rather than exact) nature of the convergence. In addition, the study is limited to simulation, and experimental validation is left for future work.

5 Conclusion

A singularity-free predefined-time sliding mode controller with a fixed-time extended state observer has been proposed for robot manipulators. By employing a predefined-time stable system with a closed-form settling-time function, the design parameters are made the least upper bounds of the convergence time, and the singularity of the sliding surface is removed by a C^1 transition function. Practical predefined-time convergence has been proved with an explicit time budget and an explicit residual set. Through simulations on a two-link manipulator, it has been shown that, compared with SMC, NTSMC, and fixed-time SMC, the prescribed time is respected by the proposed method under various initial conditions and parameter variations, comparable or better steady-state accuracy is achieved with a smooth torque, and chattering is reduced by more than four orders of magnitude relative to discontinuous fixed-time control. In future work, saturation-aware selection of the predefined times, noise-robust implementation through measurement filtering, extension to manipulators with more degrees of freedom, and experimental validation will be addressed.

References

1. Slotine JJE, Li W (1991) Applied nonlinear control. Prentice Hall, Englewood Cliffs
2. Spong MW, Hutchinson S, Vidyasagar M (2006) Robot modeling and control. Wiley, Hoboken
3. Feng Y, Yu X, Man Z (2002) Non-singular terminal sliding mode control of rigid manipulators. Automatica 38(12):2159–2167
4. Polyakov A (2012) Nonlinear feedback design for fixed-time stabilization of linear control systems. IEEE Trans Autom Control 57(8):2106–2110
5. Zuo Z (2015) Nonsingular fixed-time consensus tracking for second-order multi-agent networks. Automatica 54:305–309
6. Aldana-López R, Gómez-Gutiérrez D, Jiménez-Rodríguez E, Sánchez-Torres JD, Defoort M (2019) Enhancing the settling time estimation of a class of fixed-time stable systems. Int J Robust Nonlinear Control 29(12):4135–4148. https://doi.org/10.1002/rnc.4600
7. Sánchez-Torres JD, Gómez-Gutiérrez D, López E, Loukianov AG (2018) A class of predefined-time stable dynamical systems. IMA J Math Control Inf 35(Suppl 1):i1–i29
8. Jiménez-Rodríguez E, Muñoz-Vázquez AJ, Sánchez-Torres JD, Defoort M, Loukianov AG (2020) A Lyapunov-like characterization of predefined-time stability. IEEE Trans Autom Control 65(11):4922–4927
9. Song Y, Wang Y, Holloway J, Krstic M (2017) Time-varying feedback for regulation of normal-form nonlinear systems in prescribed finite time. Automatica 83:243–251
10. Liang CD, Ge MF, Liu ZW, Wang YW, Karimi HR (2020) Predefined-time terminal sliding mode control of robot manipulators. arXiv:2001.04198. https://arxiv.org/abs/2001.04198
11. Zhang N, Wang S, Hou Y, Zhang L (2020) A robust predefined-time stable tracking control for uncertain robot manipulators. IEEE Access 8:188600–188610. https://doi.org/10.1109/ACCESS.2020.3031328

12. Sai H, Xu Z, Zhang E (2023) Adaptive practical predefined-time neural tracking control for multi-joint uncertain robotic manipulators with input saturation. Neural Comput Appl 35(27):20423–20440. https://doi.org/10.1007/s00521-023-08797-2
13. Ahmed S, Azar AT (2025) Predefined-time fractional-order terminal SMC for robot dynamics. Int J Optim Control Theor Appl 15(3):426–434. https://doi.org/10.36922/IJOCTA025060020
14. Ye H, Liu C, Lam J, Song Y, Kwok KW, Zhou Y (2026) A nonconservative prescribed-time control approach for robotic manipulation: design and experiment. IEEE Trans Ind Electron. https://doi.org/10.1109/TIE.2026.3699870
15. Yang S, Wang Y, Yang Y, Sun G (2026) Predefined-time disturbance observer-based nonsingular sliding mode control with prescribed performance for robotic manipulators. Mathematics 14(13):2293. https://doi.org/10.3390/math14132293
16. Han J (2009) From PID to active disturbance rejection control. IEEE Trans Ind Electron 56(3):900–906
17. Andrieu V, Praly L, Astolfi A (2008) Homogeneous approximation, recursive observer design, and output feedback. SIAM J Control Optim 47(4):1814–1850
18. Basin M, Shtessel Y, Aldukali F (2016) Continuous finite- and fixed-time high-order regulators. J Franklin Inst 353(18):5001–5012. https://doi.org/10.1016/j.jfranklin.2016.09.026
19. Cruz-Zavala E, Moreno JA, Fridman LM (2011) Uniform robust exact differentiator. IEEE Trans Autom Control 56(11):2727–2733
20. Moreno JA (2020) Arbitrary order fixed-time differentiators. arXiv:2011.02012. https://arxiv.org/abs/2011.02012
21. Yang F, Wei C, Wu R, Cui N (2018) Non-recursive fixed-time convergence observer and extended state observer. IEEE Access 6:62339–62351. https://doi.org/10.1109/ACCESS.2018.2875894
22. Vo AT, Truong TN, Kang HJ, Van M (2021) A robust observer-based control strategy for n-DOF uncertain robot manipulators with fixed-time stability. Sensors 21(21):7084. https://doi.org/10.3390/s21217084
23. Vo AT, Truong TN, Le QD, Kang HJ (2023) Fixed-time sliding mode-based active disturbance rejection tracking control method for robot manipulators. Machines 11(2):140. https://doi.org/10.3390/machines11020140
24. Truong TN, Vo AT, Kang HJ, Le TD (2022) An observer-based fixed time sliding mode controller for a class of second-order nonlinear systems and its application to robot manipulators. In: Intelligent computing methodologies (ICIC 2022). Lecture Notes in Artificial Intelligence, vol 13395. Springer, Cham, pp 529–543. https://doi.org/10.1007/978-3-031-13832-4_44
25. Khalil HK (2002) Nonlinear systems, 3rd edn. Prentice Hall, Upper Saddle River
26. Levant A (2003) Higher-order sliding modes, differentiation and output-feedback control. Int J Control 76(9–10):924–941